ATPase Kinetics of Recombinant Bovine 70 kDa Heat Shock Cognate Protein and Its Amino-Terminal ATPase Domain†

Jeung-Hoi Ha and David B. McKay*

Beckman Laboratories for Structural Biology, Department of Structural Biology, Stanford University School of Medicine, Stanford, California 94305

Received June 9, 1994; Revised Manuscript Received September 8, 1994®

ABSTRACT: Steady-state kinetic, pre-steady-state kinetic, and equilibrium binding measurements have been applied to determine the rate constants of individual steps of the ATPase cycle for the recombinant bovine 70 kDa heat shock cognate protein and its amino-terminal 44 kDa ATPase fragment. At 25 °C, pH 7.0, in the presence of 75 mM KCl and 4.5 mM Mg^{2+}, the measured association rate constants for MgATP~hsc70 and MgADP~hsc70 are $(2.7 \pm 0.5) \times 10^5$ and $(4.1 \pm 0.5) \times 10^5$ M^{-1} s^{-1}, respectively, while the dissociation rate constants are 0.0114 (±0.0002) and 0.0288 (±0.0018) s^{-1}, respectively. MgATP ($K_d = 0.042$ μM) therefore binds to hsc70 more tightly than MgADP ($K_d = 0.11$ μM). ADP release is inhibited by inorganic phosphate (P_i), suggesting that product dissociation is ordered with P_i released first and ADP second. The rate of chemical hydrolysis of ATP is 0.0030 (±0.0003) s^{-1} for hsc70 and 0.0135 (±0.0033) s^{-1} for the 44 kDa fragment. The rate of P_i release is 0.0038 (±0.0010) s^{-1} for hsc70 and 0.0051 (±0.0006) s^{-1} for the 44 kDa fragment. For the 44 kDa fragment, P_i release is the slowest step in the ATPase cycle, while for hsc70, P_i release and chemical hydrolysis of MgATP have similar rates; in both cases, ADP release is a relatively rapid step in the ATPase cycle.

The bovine 70 kDa heat shock cognate protein (hsc70[1]) is a constitutively expressed member of the highly conserved family of 70 kDa heat shock-related molecular chaperone proteins, or stress-70 proteins, that are required for cell viability in all organisms [for reviews, see Gething and Sambrook (1992), Hendrick and Hartl (1993), McKay (1993), and Becker and Craig (1994)]. hsc70 was originally characterized as a clathrin uncoating ATPase (Chappell et al., 1986); it has subsequently been implicated in facilitating the transmembrane targeting of proteins (Chirico et al., 1988; Deshaies et al., 1988; Murakami et al., 1988) and is found by immunoprecipitation to be associated with nascent polypeptides during translation (Beckmann et al., 1990; Sheffield et al., 1990; Beckmann et al., 1992). It is thought that stress-70 proteins bind unstructured polypeptides *in vivo*, thereby inhibiting aggregation or misfolding (Beckmann et al., 1990; Palleros et al., 1991). MgATP is utilized to drive the release of bound polypeptides. *In vitro*, stress-70 proteins bind short (≥7 residue) peptides (Flynn et al., 1991; Landry et al., 1992; Blond-Elguindi et al., 1993) and denatured proteins (Beckmann et al., 1990; Liberek et al., 1991b; Palleros et al., 1991); peptide binding/release is coupled to the ATPase cycle in such a manner that excess MgATP induces peptide release, and reciprocally, high concentrations of peptide stimulate the steady-state ATPase activity severalfold above its basal level. Additionally, the ATPase activity of some stress-70 proteins is known to be modulated by accessory proteins; for example, the activity of *Escherichia coli* dnaK protein can be stimulated ~50-fold *in vitro* by the concerted actions of *E. coli* dnaJ and grpE proteins (Liberek et al., 1991a).

The ATPase activity of hsc70 is localized in the amino-terminal ~385 amino acid residues of the molecule (Chappell et al., 1987; Milarski & Morimoto, 1989; Flaherty et al., 1990); isolation of this 44 kDa amino-terminal fragment, either by proteolysis of full-length hsc70 or by recombinant expression of a truncated molecule, yields a construct with a peptide-independent ATPase activity. The peptide binding activity of hsc70 is located within the carboxy-terminal remainder of the molecule. The 44 kDa fragment has been crystallized and its three-dimensional structure has been solved (Flaherty et al., 1990); the structure is strikingly similar to that of actin (Flaherty et al., 1991; Bork et al., 1992). The crystallographic structure revealed several residues in the active site region of the 44 kDa fragment that might participate in ATPase activity. These residues have been mutated, and both the crystallographic structures and the steady-state, multiple-turnover ATPase kinetics of these point mutants have been reported (Gaut & Hendershot, 1993; Huang et al., 1993; O'Brien & McKay 1993; Flaherty et al., 1994; Wilbanks et al., 1994). These results have suggested a chemical mechanism for MgATP hydrolysis (Flaherty et al., 1994; Wilbanks et al., 1994). The 44 kDa fragment is a convenient construct that allows one the opportunity to study the kinetics and mechanism of the ATPase reaction decoupled from peptide binding and release; by comparison, full-length hsc70 then can be considered to be a similar ATPase, with added complexity introduced by the peptide binding activity and its coupling to the ATPase cycle.

† Supported by NIH Award GM-39928 to D.B.M.

* Author to whom correspondence should be addressed.

® Abstract published in *Advance ACS Abstracts,* November 15, 1994.

[1] Abbreviations: kDa, kilodalton; hsc70, 70 kDa heat shock cognate protein; EDTA, ethylenediaminetetraacetic acid; HEPES, *N*-(2-hydroxyethyl)piperazine-*N*′-2-ethanesulfonic acid; BSA, bovine serum albumin; MOPS, 3-morpholinopropanesulfonic acid; $Mg(OAc)_2$, $Mg(CH_3COOH)_2$; AMPPNP, imidoadenosine 5′-triphosphate; P_i, orthophosphate; TCA, trichloroacetic acid; TLC, thin-layer chromatography.

0006-2960/94/0433-14625$04.50/0

The steady-state ATPase activity of stress-70 proteins is relatively slow, with turnover rates ranging from 0.0004 to 0.017 s^{-1} having been reported for members of the family [Wilbanks et al., 1994; for other references, see McKay et al. (1994)]. Several proposals have been made regarding the mechanism of coupling of the ATPase activity with peptide binding and release (Schlossman et al., 1984; Palleros et al., 1993; Prasad et al., 1994; Schmid et al., 1994). The clathrin uncoating activity of hsc70 was shown to require MgATP; the nonhydrolyzable analog [γ-S]ATP did not support clathrin disassembly (Schmid & Rothman, 1985). This observation led to the suggestion that MgATP hydrolysis is required for an essential step in the clathrin uncoating reaction. Consistent with the suggestion that MgATP hydrolysis may be a critical step was the later observation that MgATP induced a conformational change and release of denatured proteins in dnaK, while the nonhydrolyzable analog MgAMPPNP failed to do so (Liberek et al., 1991b). In contrast, recent evidence has been presented to support a model in which MgATP binding induces the rapid release of denatured proteins prior to hydrolysis by dnaK and other stress-70 proteins (Palleros et al., 1993; Prasad et al., 1994).

It has also been demonstrated that a representative denatured protein substrate, apocytochrome *c*, stimulates the release rate of ADP by hsc70 (Sadis & Hightower, 1992), suggesting that unfolded polypeptides stimulate the ATPase rate of hsc70 by accelerating ATP/ADP exchange; this raises the question of what role nucleotide exchange plays in regulating peptide binding and release by stress-70 proteins.

Ultimately, delineation of the biochemical coupling of the ATPase cycle with the peptide binding/release cycle, as well as an understanding of the mechanism of modulation of ATPase activity by accessory proteins, will require a detailed kinetic description of the enzymatic cycle, to wit a description of the reaction pathway and the rate constants of the individual steps. Such a description is not currently available. Toward this end, we have used equilibrium binding, steady-state kinetics, and pre-steady-state kinetics to determine the reaction pathway and the rates of the individual steps of the ATPase cycle for recombinant bovine hsc70 and its 44 kDa fragment.

EXPERIMENTAL PROCEDURES

Protein Expression and Purification. Recombinant wild-type hsc70 and its amino-terminal 44 kDa ATPase fragment were expressed in *E. coli* and purified as described previously (O'Brien & McKay, 1993). Nucleotide-free proteins were prepared as follows: Protein was mixed with 1 mg/mL activated charcoal (Mallinckrodt) in 10 mM Na_2EDTA, adjusted to pH 8.0 with KOH, and gently shaken at 4 °C for 4 h. The charcoal was removed by centrifugation, and the supernatant was dialyzed extensively against 40 mM HEPES and 4.5 mM $Mg(OAc)_2$ and adjusted to pH 7.0 with KOH. Protein concentration was determined from the optical absorbance at 280 nm using the extinction coefficients 30 820 M^{-1} cm^{-1} for hsc70 and 18 610 M^{-1} cm^{-1} for the 44 kDa fragment, calculated from the amino acid compositions (Genetics Computer Group programs, Madison, WI). More than 95% of the protein was nucleotide-free. MgATP/MgADP binding activity of nucleotide-free proteins was tested using a filter binding assay under stoichiometric binding conditions; protein preparations were ~100% active in nucleotide binding. The ATPase activity of nucleotide-free proteins is unstable at submicromolar concentrations; however, the addition of 50 μg/mL bovine serum albumin (BSA) stabilized the activities of both hsc70 and the ATPase fragment at 37 °C to concentrations as low as 20 nM.

Preparation of [α-^{32}P]ADP. To prepare labeled ADP, 42 pmol of [α-^{32}P]ATP (Amersham) was combined with 0.4 unit of hexokinase (Sigma) and 3 mM glucose in 40 mM HEPES (pH 7.0), 50 mM KOAc, 5 mM $Mg(OAc)_2$, and 5 mM dithiothreitol and incubated at 25 °C for 45 min. Within 3 min, more than 90% of the ATP was converted to ADP; after 45 min the reaction had gone to completion. The solution was diluted 20-fold with 0.02 M NH_4OAc and applied to a DEAE-Sephadex A-25 column. [α-^{32}P]ADP was eluted with a 0.02−0.5 M NH_4OAc gradient and was further purified by passage through a SEP-PAK C_{18} cartridge (Waters-Millipore) equilibrated with H_2O. NH_4OAc was removed by evaporation in a SpeedVac concentrator.

Determination of Kinetic Parameters. Kinetic experiments were carried out in 40 mM HEPES, 4.5 mM $Mg(OAc)_2$, 75 mM KCl, and 50 μg/mL BSA, adjusted to pH 7.0 with KOH prior to the addition of BSA, unless otherwise stated; this is referred to as the 75 mM KCl buffer. For comparison to results in the literature, in some cases measurements were made in 25 mM KCl and 10 mM $(NH_4)_2SO_4$; this is referred to as the 25 mM KCl/10 mM $(NH_4)_2SO_4$ buffer. A filter binding protocol was used to measure the retention of radiolabeled ligands by protein: Schleicher and Schuell BA-85 nitrocellulose filters were soaked in 0.4 M KOH for 10 min, washed extensively with deionized water, and equilibrated with a wash buffer consisting of the 75 mM KCl buffer with the omission of BSA. Samples of 10−45 μL were spotted onto the filters and washed with 0.6 mL of wash buffer; control experiments demonstrated that over the range 0.5−1.0 mL, the volume of wash buffer used did not affect the total counts retained on the filter. Filters were dried and Cerenkov radiation was counted by using a Beckman LS 5000TA scintillation counter. The filter binding efficiency of the proteins was typically 90% ± 10% for hsc70 and 45% ± 10% for the 44 kDa fragment.

Hydrolysis of [α-^{32}P]ATP was monitored by separating ADP from ATP with thin-layer chromatography (TLC) on poly(ethylene imine)−cellulose, using methods described previously (O'Brien & McKay, 1993), and quantitating the relative amounts of [α-^{32}P]ADP and [α-^{32}P]ATP as radioactive counts from their respective TLC spots, measured with a phosphorimager system (Molecular Dynamics). The boundaries of the TLC spots were outlined with a rectangular grid. For each cell in the grid, the background intensity level of the phosphorimager plate was set equal to the average counts per pixel on the cell border, and this value was subtracted from each pixel within the cell. Typically, the sum of integrated intensities for a pair of spots (substrate ATP plus product ADP) was $N \sim 10^6$ counts. The ADP produced ranged over 1−100% of the sample, so that the smallest integrated intensities were typically 10^4 counts, and the maximum corresponding relative statistical error of the intensity measurement was $(N)^{1/2} \sim 10^2$ counts, or ~1%. At the highest salt concentrations used, some spots showed streaks; however, these accounted for <5% of the total intensity of the spots and generally could be included within the integration boundaries. In a series of tests, wherein rectangular boxes of different sizes were used for spot

integration, it was found that although the values of the integrated counts showed some variation with the size of the integration area, the fraction of ATP hydrolyzed at each time point and the rate constants computed from these values agreed within statistical error for different integration boxes. Data were analyzed using the nonlinear least-squares utility of the Enzfit software (Elsevier/Biosoft) unless stated otherwise. Calculations performed in parallel with other software packages (KaleidaGraph) or in-house programs gave results that agreed within estimated standard deviations with those of Enzfit. The uncertainty reported is the standard error of a least-squares fit.

The apparent rate of association of MgATP with hsc70 was determined by filter binding. Stock solutions of nucleotide-free hsc70 at four concentrations ranging over 40−320 nM were prepared and preincubated at 25 °C for 2 min. The binding reaction was initiated by mixing equal volumes of the protein solution and a [α-^{32}P]ATP solution that had been preequilibrated at 25 °C for 5 min. The final concentration of ATP after mixing was 1 nM. For each sample, 10 time points were taken during a 180 or 240 s period. The fraction of substrate bound to protein was computed as $\theta = (C - C_B)/(C_T - C_B)$, where C is the total counts retained on the filter, C_B is the background counts retained when ATP is filtered without protein, and C_T is the total input counts. The apparent association rate constant, k_a, was computed by fitting a single exponential of the form $\theta_{t\to\infty}(1 - \exp(-k_a t))$ to the fraction of background-corrected counts retained on filters (θ) versus time, where $\theta_{t\to\infty}$ is the asymptotic value of the function. The apparent rate of association of MgADP with hsc70 was determined in a similar manner, using hsc70 concentrations ranging over 40−160 nM.

Filter binding experiments were also used to determine the rates of dissociation of ADP from hsc70 and the 44 kDa ATPase fragment. A stoichiometric complex was formed by incubating a mixture of 2 μM [α-^{32}P]ATP and 2 μM hsc70 or 44 kDa ATPase fragment at 37 °C for 30 min to allow essentially complete hydrolysis to MgADP and then transferring it to a 25 °C bath. The complex was purified from free nucleotide and P_i by gel filtration on Sephadex G-25 (Pharmacia NICK column). Unlabeled ADP (Sigma) was added to final concentrations ranging from 0 to 0.4 mM to block the reassociation of released [α-^{32}P]ADP, and the decrease in protein-bound radioactivity was measured as a function of time by filter binding. The apparent dissociation rate was calculated by fitting a single exponential to the time course of the decay. The effect of [P_i] on the rate of ADP release by the 44 kDa fragment was determined with essentially the same protocol, but with the additional inclusion of P_i from KH_2PO_4 at concentrations ranging from 0.001 to 0.1 M in the reaction mixtures, with the pH adjusted to 7.0 in all experiments. A separate set of experiments was performed with hsc70 under similar conditions, except that [α-^{32}P]ADP was used rather than [α-^{32}P]ATP; in this case, it was not necessary to incubate the complex to allow nucleotide hydrolysis before adding unlabeled ADP.

The rate of MgATP hydrolysis was measured under single-turnover conditions, with enzyme present in substantial molar excess over MgATP. Protein and [α-^{32}P]ATP solutions were preincubated separately at 25 °C for 2 and 5 min, respectively, and then mixed; the final concentration of ATP was 10 nM, and that of the protein ranged from 0.05 to 1.60 μM. Aliquots of the reaction solution were removed and mixed with an equal volume of ice-cold 12% trichloroacetic acid (TCA); the acid-quenched solution was then rapidly neutralized by the addition of 2.1× volumes of 10 mM MOPS and 0.4 M KOH; this resulted in a final pH of 7 for the mixture. ADP and ATP were separated by TLC and quantitated with a phosphorimager as described earlier. The fraction of ATP converted to product ADP was computed as $\phi = N_{ADP}/(N_{ADP} + N_{ATP})$ for each time point, where N_{ADP} and N_{ATP} are the total counts after background subtraction in the ADP and ATP spots of the TLC plate, respectively. The observed single-turnover hydrolysis rate constant, k^{st}, was computed by fitting a single exponential of the form, $\phi_{t=\infty}(1 - \exp(-k^{st}t)) + \phi_{t=0}$, to the data on the fraction of nucleotide converted to ADP versus time, where $\phi_{t=0}$ and $\phi_{t=\infty}$ are the mangitudes of ϕ at zero time and at an asymptotic end point, respectively. K_M and k_{cat} were calculated by a weighted nonlinear least-squares fit of the function

$$k^{st} = \frac{k_{cat}[\text{protein}]}{K_M + [\text{protein}]} \quad (1)$$

to the values of k^{st} versus protein concentration; validation of the use of this function is discussed under Results. K_M and k_{cat} obtained from single-turnover kinetics with [α-^{32}P]-ATP are denoted as K_M^{st} and k_{cat}^{st}.

Experiments were also performed under single-turnover conditions to measure the rate of release of radioactive label when [γ-^{32}P]ATP is used as the substrate. [ATP] was held constant at 10 nM, and the concentration of protein was varied from 3.0 to 14.1 μM; the lowest protein concentration was therefore substantially greater than $K_d \sim 10^{-7}$ M for the protein−MgATP and protein−MgADP complexes for both hsc70 and the 44 kDa fragment, resulting in saturation of the nucleotide with protein after mixing. Aliquots were filtered at times ranging from 0 to 4000 s; the counts retained on the filter represent the radioactive label retained as either [γ-^{32}P]ATP or $^{32}P_i$. Values of the P_i off-rate were estimated by fitting a function with two exponential terms, one of which had a decay constant equal to the hydrolysis rate, to the fraction of background-corrected counts retained on the filter (θ) as a function of time (discussed more extensively under Results).

Steady-state parameters for the ATPase activity at 25 °C were determined with methods described previously (O'Brien & McKay, 1993; Wilbanks et al., 1994). The final protein concentrations in the reaction mixtures were 0.42 μM for hsc70 and 0.02 μM for the 44 kDa. The ATP concentration ranged from 9 to 96 μM for hsc70 and from 0.2 to 6.4 μM for the 44 kDa fragment. For the 44 kDa fragment, K_M and k_{cat} were obtained from a weighted nonlinear least-squares fit of the Michaelis−Menten equation,

$$k_{obs} = \frac{k_{cat}[\text{ATP}]}{K_M + [\text{ATP}]} \quad (2)$$

to the data of k_{obs} (the initial velocity divided by the concentration of protein) versus ATP concentration. hsc70 was assayed under maximum velocity conditions, giving only k_{cat}. K_M and k_{cat} obtained from steady-state kinetics were denoted as K_M^{ss} and k_{cat}^{ss}. For hsc70, only k_{cat}^{ss} was determined.

Determination of the Equilibrium Binding Constants for MgADP−Protein Complexes. The equilibrium dissociation

Table 1: Kinetic Parameters for the ATPase Cycle[a]

parameter	hsc70	44 kDa fragment
k_1 (M^{-1} s^{-1})	(2.69 ± 0.46) × 10^5	nd[b]
k_{-1} (s^{-1})	0.0114 (±0.0002)	nd[b]
k_2 (s^{-1})	0.0030 (±0.0003)	0.0135 (±0.0033)
k_3 (s^{-1})	0.0038 (±0.0010)	0.0051 (±0.0006)
k_4 (s^{-1})	0.0288 (±0.0018)	0.0347 (±0.0016)
k_{-4} (M^{-1} s^{-1})	(4.1 ± 0.5) × 10^5	nd[b]
k_{-4}^{calcd} [= k_4/K_d(ADP)] (M^{-1} s^{-1})	(2.6 ± 0.5) × 10^5	(3.7 ± 0.5) × 10^5
k_{cat}^{ss} (s^{-1})	0.0012 (±0.00002)	0.0023 (±0.0002)
K_M^{st} (μM)	0.25 (±0.05)	0.65 (±0.34)
K_M^{ss} (μM)	nd[b]	0.37 (±0.09)
K_d(ADP) (μM)	0.11 (±0.02)	0.094 (±0.012)
K_d^{calcd}(ATP) [=k_{-1}/k_1] (μM)	0.042 (±0.007)	nd[b]

[a] Parameters are as defined in the text. Values were determined at 25 °C in 40 mM HEPES, 4.5 mM $Mg(OAc)_2$, 75 mM KCl, and 50 μg/mL BSA, adjusted to pH 7.0. The superscript calcd denotes that the value was computed from constants that were determined experimentally, as described in text; ss denotes steady state; st denotes single turnover. The definitions of computed constants are enclosed in square brackets. [b] Not determined.

Scheme 1

$$E \underset{k_{-1}}{\overset{k_1[ATP]}{\rightleftharpoons}} E\text{–}ATP \underset{k_{-2}}{\overset{k_2}{\rightleftharpoons}} E\text{–}ADP\text{–}P_i \underset{k_{-3}[P_i]}{\overset{k_3}{\rightleftharpoons}} E\text{–}ADP \underset{k_{-4}[ADP]}{\overset{k_4}{\rightleftharpoons}} E$$

constants (K_d) for complexes of MgADP with hsc70 and the 44 kDa fragment were determined with filter binding. In one set of experiments, protein at concentrations from 20 nM to 2.56 μM was incubated with 1 nM [α-^{32}P]ATP for 2.5 h at 25 °C to allow complete hydrolysis of the nucleotide. The solution was then filtered, and K_d and the filter efficiency E were determined by a least-squares fit of the equation:

$$\theta = \frac{[\text{protein}]}{[\text{protein}] + K_d} E \qquad (3)$$

to the data on the fraction of background-corrected counts retained on the filter (θ) as a function of protein concentration. As an independent confirmation, a second set of experiments was done with hsc70, in which essentially the same method was used with the substitution of [α-^{32}P]ADP for [α-^{32}P]ATP; in this case, extended incubation of the solutions to allow nucleotide hydrolysis was unnecessary.

RESULTS

We have interpreted our results with Scheme 1. This scheme assumes an ordered release of products, with P_i released before ADP; experimental data will be presented here that justify this approximation for the kinetic data presented.

ADP Off-Rates and Equilibrium Binding Constants. The rate of [α-^{32}P]ADP release (k_4; Scheme 1) was determined by filter binding for both hsc70 and the 44 kDa ATPase fragment as described in The Experimental Procedures. [α-^{32}P]ADP–protein complexes were formed by incubating protein with [α-^{32}P]ATP for long enough to allow complete hydrolysis, followed by gel filtration. Off-rate measurements were initiated by adding a large molar excess of cold ADP; in the absence of cold ADP, no net dissociation of [α-^{32}P]-ADP from a 2 μM protein–nucleotide complex was observed, presumably because of the tight ($\leq 10^{-7}$ M) binding

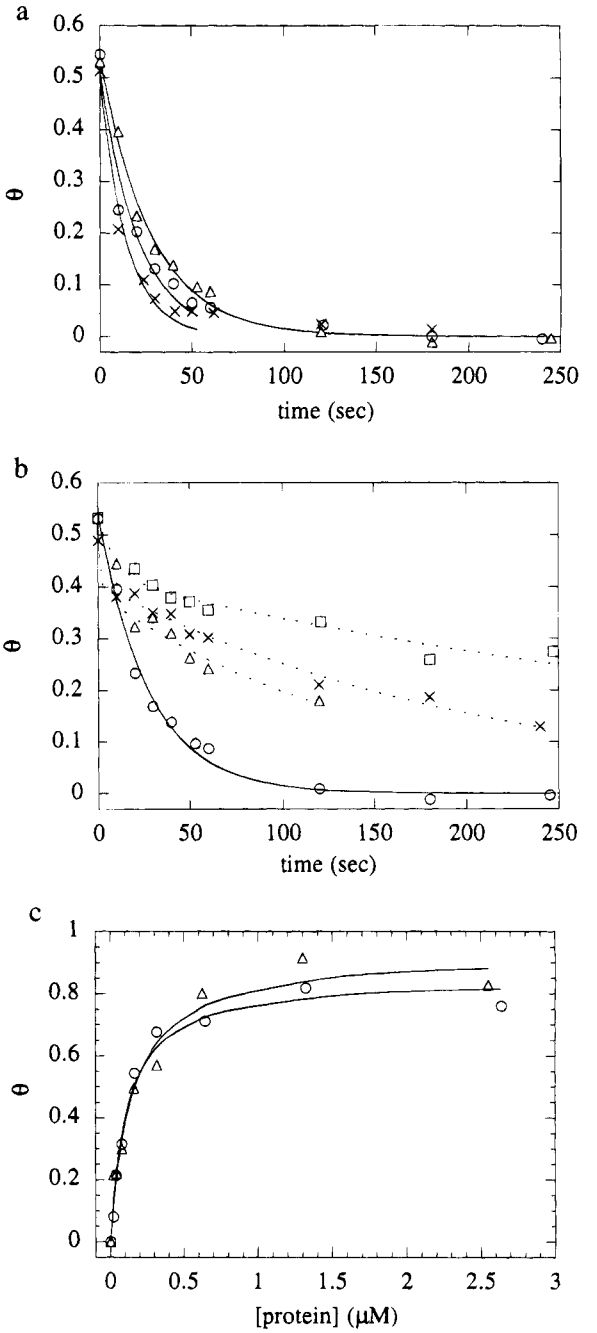

FIGURE 1: ADP dissociation and equilibrium binding. θ denotes the fraction of background-corrected radioactive counts retained on the filter. (a) Dissociation kinetics of ADP from the 44 kDa ATPase fragment at 2 μM P_i and variable KCl. Symbols are as follows: (△) 0.075 M KCl; (○) 0.2 M KCl; (×) 0.8 M KCl. Curves represent nonlinear least-squares fit of a single-exponential decay to the data on θ versus time. (b) Dissociation kinetics of ADP from its complex with the 44 kDa fragment showing the effect of P_i concentration. Solution conditions (all adjusted to pH 7.0) are as follows: (○) 2 μM P_i and 0.075 M KCl; (△) 0.001 M potassium phosphate and 0.073 M KCl; (×) 0.01 M potassium phosphate and 0.055 M KCl; (□) 0.1 M potassium phosphate. Dashed curves are drawn for clarity and do not represent the fit of a function to the data. (c) Equilibrium binding curves for MgADP with (△) hsc70 and (○) the 44 kDa ATPase fragment. Curves are the results of nonlinear least-squares fits of a hyperbolic function in θ versus protein concentration (eq 3) to the data.

of MgADP under these conditions. The rate of dissociation of ADP from the ATPase fragment (Figure 1a) and hsc70 showed only a modest dependence on the KCl concentration; increasing [KCl] from 0.075 to 0.8 M approximately doubled

the off-rate. The rate of ADP release was independent of the concentration of unlabeled ADP added over the range 0.1−1.0 mM (data not shown), indicating that ADP release follows first-order kinetics. ADP is released at a similar rate from hsc70 and from the 44 kD fragment, with measured off-rates of 0.0288 (±0.0018) s^{-1} for hsc70 and 0.0347 (±0.0016) s^{-1} for the 44 kDa fragment. To check consistency, the off-rate for hsc70 was also measured by this method using [α-^{32}P]ADP as the starting nucleotide; a value of 0.051 (±0.007) s^{-1} was obtained, which agrees reasonably well with the value determined using [α-^{32}P]ATP as the nucleotide and allowing complete hydrolysis before the measurement. For comparison to other values reported in the literature, we also measured the ADP off-rate for hsc70 in 25 mM KCl/10 mM $(NH_4)_2SO_4$ buffer and obtained a value of 0.024 (±0.004) s^{-1}; within error, this is equal to the value obtained in 75 mM KCl buffer.

Measurement of the rate of release of [α-^{32}P]ADP in the presence of exogenous potassium phosphate in the range 0.001−0.1 M shows that ADP release is inhibited by sufficiently high concentrations of this salt (Figure 1b). The inhibitory effect of potassium phosphate on ADP release is not due to K^+, since the effect of K^+ in the form of KCl over this concentration range is to modestly increase the rate of ADP release (Figure 1a). The inhibitory effect therefore depends on P_i. The rate of release of [α-^{32}P]ADP was not affected by exogenous [P_i] ≤ 50 μM (data not shown). The maximum P_i concentration that could be generated from ATP in the ADP release experiments is 2 μM, which would not affect the rate of ADP release. However, in the range 0.001−0.1 M added P_i, the rate of ADP release is reduced severalfold and no longer follows a single-exponential decay. This argues in favor of an ordered release of products, with P_i leaving first and ADP second; if release of the two products was independent of each other, or if ADP dissociated before P_i, the ADP off-rate should be independent of [P_i]. Hence, we are using the approximation of ordered product release in our description of the ATPase cycle for both hsc70 and the ATPase fragment (Scheme 1). [Parenthetically, it should be noted that at the higher concentrations of P_i, the concentration of free Mg^{2+} will be reduced from the exogenous level of 4.5 mM. The K_d for $MgHPO_4$ is ~3 × 10^{-3} M (O'Sullivan, 1969), so that at 0.1 M P_i, the free Mg^{2+} will be ~0.1 mM. The [Mg^{2+}] dependence of the ATPase activity of the wild-type 44 kDa fragment has been reported and shows a $K_M(Mg^{2+})$ ≤ 0.01 mM (Wilbanks et al., 1994), so that in the range 0.001−0.1 M P_i, free [Mg^{2+}] is still high enough to support essentially full ATPase activity].

The equilibrium dissociation constants for MgADP complexed with hsc70 and the 44 kDa fragment were determined using the filter binding assay with protein in large excess (20 nM to 2.56 μM) over nucleotide (1 nM), as described under Experimental Procedures. The fraction of [α-^{32}P]ADP retained on filters as a MgADP−protein complex was determined as a function of the protein concentration (Figure 1c). Fitting a hyperbolic curve to these data gives the binding constants: for hsc70, K_d is 0.11 (±0.02) μM, and for the 44 kDa fragment, K_d is 0.094 (±0.012) μM. The maximum concentration of P_i generated under these conditions is 1 nM, which should have a negligible effect on the K_d, since concentrations substantially greater than 50 μM would be required for an observable effect on the ADP off-rate.

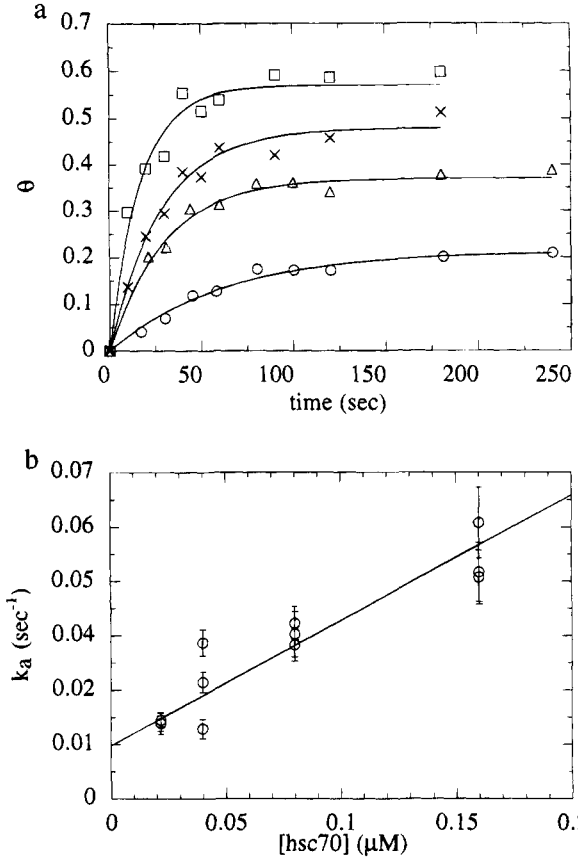

FIGURE 2: Association kinetics of MgATP with hsc70. (a) Plots of θ, the fraction of counts retained on the filter, as a function of time for different concentrations of hsc70: (○) 22 nM; (△) 40 nM; (×) 80 nM; (□) 160 nM. Curves represent nonlinear least-squares fits of a single exponential to measured values of θ versus time. (b) Plot of k_a as a function of the concentration of hsc70. The line is the result of a weighted least-squares linear fit to the data.

Determination of K_d of MgADP for hsc70 (i) using [α-^{32}P]-ATP as the nucleotide and allowing complete hydrolysis and (ii) using [α-^{32}P]ADP as the nucleotide gave identical values for the dissociation constant.

From K_d and k_4, the association rate constant of MgADP (k_{-4}) can be calculated as $k_{-4}^{calcd} = k_4/K_d$. MgADP binds at similar rates to both hsc70 and the 44 kDa fragment, with computed rate constants of (2.6 ± 0.5) × 10^5 M^{-1} s^{-1} for hsc70 and (3.7 ± 0.5) × 10^5 M^{-1} s^{-1} for the 44 kDa fragment.

ATP On- and Off-Rates. The association and dissociation rate constants (k_1 and k_{-1}, respectively; Scheme 1) of ATP were determined with hsc70 using the filter binding assay. At sufficiently low protein and nucleotide concentrations, MgATP binding to hsc70 is slow enough to be monitored with manual mixing and filtering. Representative data showing the time dependence of association of [α-^{32}P]ATP with hsc70 are shown in Figure 2a. Increasing the hsc70 concentration increases the observed, or apparent, rate constant of MgATP binding (k_a). The dependence of k_a on the hsc70 concentration (Figure 2b) is expected to be linear, with the form

$$k_a = k_{-1} + k_1[\text{hsc70}] \quad (4)$$

Under the conditions that initial MgATP binding is at rapid equilibrium and that the hydrolysis of MgATP is insignificant, the intercept of the line yields k_{-1}. The slope of the

linear fit yields $k_1 = (2.69 \pm 0.46) \times 10^5$ M^{-1} s^{-1}. Extrapolation to zero protein concentration gives an intercept equal to $k_{-1} = 0.0114$ (± 0.0002) s^{-1}. The amount of MgATP hydrolyzed in these experiments was measured and found to be less than 10% of the total MgATP amount at the highest protein concentrations and substantially lower at the lower protein concentrations, so that extrapolation to zero protein concentration should give a reliable estimate of k_{-1} from the intercept. The equilibrium dissociation constant for MgATP can be computed as $K_d^{calcd} = k_{-1}/k_1 = 0.042$ (± 0.007) μM, which is approximately 2-fold lower than the experimentally determined dissociation constant for the MgADP−hsc70 complex.

MgATP binding to the 44 kDa fragment showed an initial step that was significantly more rapid than that observed for hsc70, followed by a slower phase. The time dependence of the binding under the experimental conditions tested could not be analyzed accurately with a single exponential, due to the initial rapid phase; as a consequence, we do not include a quantitative analysis of MgATP binding to the 44 kDa fragment here.

ADP On-Rate. The association rate constant of MgADP as [α-^{32}P]ADP (k_{-4} of Scheme 1) for hsc70 was measured using the methods described in the previous section for determining [α-^{32}P]ATP association and dissociation rate constants. Apparent association rates were measured for the hsc70 concentration range 40−160 nM (data not shown) and analyzed as described earlier. This gave an experimental value of $k_{-4} = (4.1 \pm 0.5) \times 10^5$ M^{-1} s^{-1}. These experiments also gave an independent estimate of the dissociation rate for MgADP, $k_4 = 0.031$ (± 0.005) s^{-1}, which is in good agreement with the value determined by following the release of ADP directly (described earlier).

Hydrolysis Rate of MgATP. The rate of chemical hydrolysis of MgATP to MgADP and P_i was determined under single-turnover conditions, in which enzyme is present in large molar excess over substrate, with [α-^{32}P]ATP as a substrate. The end point of the reactions ($t \rightarrow \infty$) approaches 90% ± 10% MgADP, with the residual counts being due to nonspecific background (data not shown), demonstrating that the hydrolysis goes to completion and the rate of MgATP resynthesis from MgADP and P_i (k_{-2}) is negligible in comparison to the rate of P_i release. Independent experiments have confirmed that the rate of synthesis of MgATP from MgADP and $^{32}P_i$ is minimal (S. M. Wilbanks and D. B. McKay, unpublished results). For the case in which $k_{-2} \approx 0$ in the reaction scheme (Scheme 1), the pre-steady-state rate of formation of MgADP from MgATP will have two time-dependent terms in the form (Johnson, 1986)

$$[\mathrm{ADP}](t) = C\left(1 - \frac{\lambda_2 e^{-\lambda_1 t} - \lambda_1 e^{-\lambda_2 t}}{\lambda_2 - \lambda_1}\right) \quad (5)$$

where C is a proportionality constant, and λ_1 and λ_2 are the two solutions of the equation

$$\lambda^2 - \lambda(k_1[\mathrm{E}] + k_{-1} + k_2) + k_1 k_2 [\mathrm{E}] = 0 \quad (6)$$

in which [E] is the enzyme concentration. In the case considered here, for the protein concentrations used,

$$\lambda_1 \approx \frac{k_2[\mathrm{E}]}{[\mathrm{E}] + K_M^{st}} \quad (7)$$

$$\lambda_2 \approx k_1([\mathrm{E}] + K_M^{st}) \quad (8)$$

where

$$K_M^{st} = \frac{k_2 + k_{-1}}{k_1} \quad (9)$$

Over the range of protein concentrations used, $\lambda_2 \geq 25\lambda_1$ for hsc70; if we assume that the MgATP binding constant for the 44 kDa fragment is on the same order as that for hsc70, then $\lambda_2 \geq 2.5\lambda_1$ for the 44 kDa fragment. In both cases, the first time-dependent term of eq 5 dominates, having both a substantially larger amplitude and a substantially longer decay time than the second term, giving

$$[\mathrm{ADP}](t) \approx C(1 - e^{-\lambda_1 t}) \quad (10)$$

so that the time course of MgADP formation can be fit with a single exponential and the dependence of the apparent hydrolysis rate on enzyme concentration will be hyperbolic, as shown in Figure 3a,b for hsc70 and the 44 kDa ATPase fragment, respectively. These approximations are most accurate at high enzyme concentrations and least accurate at low enzyme concentrations, where the substrate binding rate is slowest. Hence, the asymptotic values of the hyperbolic fits to the data (k_2) are expected to be more accurate than the K_M^{st} values. The apparent K_M^{st} values for these data are larger than the values calculated from k_1, k_{-1}, and k_2; we attribute this primarily to the inaccuracy of the approximations in the range of lower protein concentrations.

It is notable that the rate of MgATP hydrolysis is substantially slower for hsc70, compared to the 44 kDa ATPase fragment, over all of the protein concentrations studied. Values of k_2 derived from these data are 0.0030 (± 0.0003) s^{-1} for hsc70 and 0.0135 (± 0.0033) s^{-1} for the 44 kDa fragment; MgATP is hydrolyzed approximately 4 times more rapidly by the 44 kDa ATPase fragment than by hsc70. Similar experiments were carried out to determine the rate of hydrolysis in the 25 mM KCl/10 mM $NH_4(SO_4)_2$ buffer; under these conditions, k_2 is 0.000 66 (± 0.000 11) s^{-1} for hsc70 and 0.0036 (± 0.0030) s^{-1} for the 44 kDa fragment. Both of these numbers are approximately 4-fold smaller than the corresponding values of k_2 determined in 75 mM KCl buffer.

Rate of P_i Release. The rate of release of the radioactive label from the protein when [γ-^{32}P]ATP is used as a substrate under single-turnover conditions was measured by filter binding, as described in the Experimental Procedures. Under the conditions employed, the slowest rate of formation of the protein−MgATP complex is $\sim k_1[\mathrm{hsc70}]_{min} \approx (3 \times 10^5$ M^{-1} $s^{-1})(3 \times 10^{-6}$ M) ≈ 1 s^{-1}, which is rapid compared to both the hydrolysis rates and the measured release rates for the radioactive label in this experiment. Also, $[\mathrm{hsc70}]_{min}$ is approximately 30-fold higher than K_d for MgATP, so that the nucleotide should be saturated with protein; parallel experiments using [α-^{32}P]ATP demonstrated that essentially all of the nucleotide was in fact bound to the protein during the experiments. Under the conditions employed, therefore, binding of MgATP is rapid relative to MgATP hydrolysis

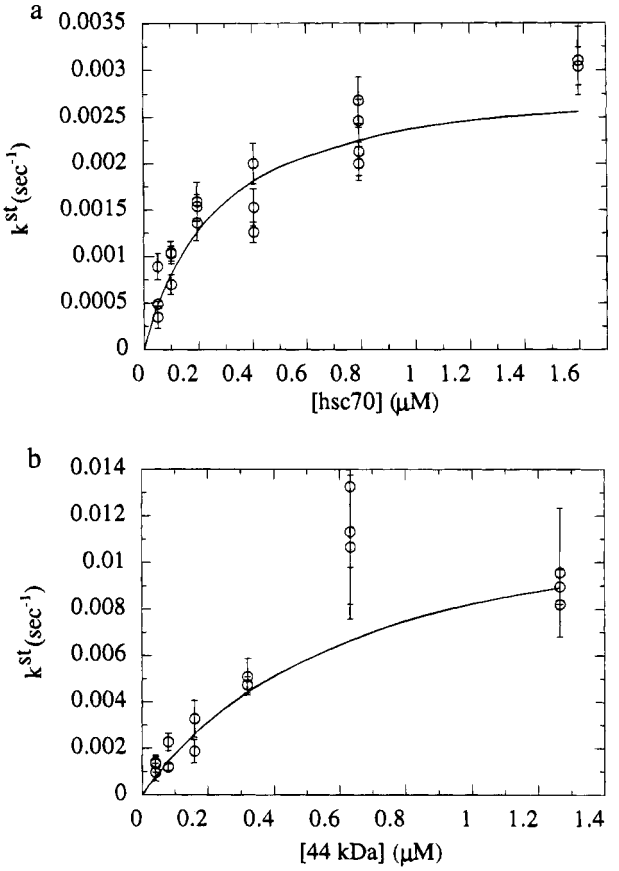

FIGURE 3: Single-turnover kinetics for MgATP hydrolysis. Dependence of the k^{st} of MgATP hydrolysis as determined in single-turnover experiments as a function of protein concentration. The uncertainty associated with k^{st} is the standard error of a nonlinear least-squares fit of a single exponential of the form described in the Experimental Procedures to the data. Curves represent weighted nonlinear least-squares fits of a hyperbolic function (eq 1) to the measured rate constants versus protein concentration. (a) k^{st} determined for hsc70 with [α-^{32}P]ATP as a substrate. (b) k^{st} determined for the 44 kDa fragment with [α-^{32}P]ATP as a substrate.

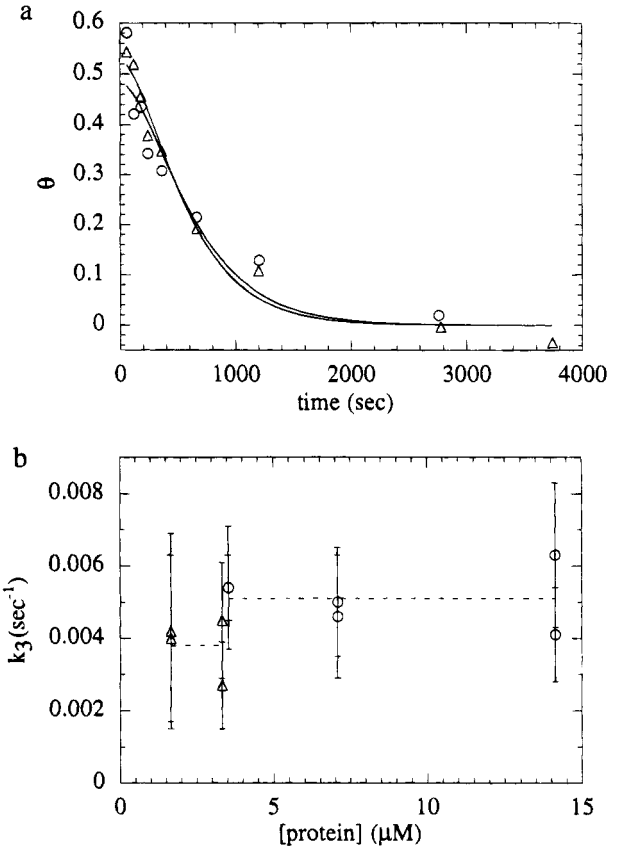

FIGURE 4: P_i release under single-turnover conditions. (a) Time dependence of the fraction of background-corrected radioactive counts retained on the filter (θ) determined with [γ-^{32}P]ATP and the following concentrations of hsc70: (△) 3.33 μM hsc70; (○) 1.66 μM hsc70. Curves represent nonlinear least-squares fits of the function (eq 11) with two time-dependent exponential terms, using the experimental values of k_2 as one rate constant, to values of θ versus time, as described in the text. (b) k_3 determined for hsc70 (△) and the 44 kDa fragment (○) as a function of protein concentration. The uncertainty associated with k_3 is the standard error of the fit of θ versus time with the function described. Lines represent the average values of k_3.

and P_i release, and the net release of radioactivity corresponds to the release of P_i. As shown in Figure 4a, the fraction of counts retained on filters asymptotically approaches zero as a function of time; it is apparent that the maximum final concentration of free P_i, ~10 nM, must be well below its equilibrium binding constant. Under these conditions, $k_{-3}[P_i] \ll k_3$, so that the rate of release of radioactive label from the filters can be parametrized as

$$\theta(t) = C\left(\frac{k_2 e^{-k_3 t} - k_3 e^{-k_2 t}}{k_2 - k_3}\right) \qquad (11)$$

The data were fit with this function, using the previously determined values of k_2, for both hsc70 and the 44 kDa fragment (Figure 4a). Values derived for k_3 determined by this method are independent of the protein concentration (Figure 4b) and are equal to 0.0038 (±0.0010) s^{-1} for hsc70 and 0.0051 (±0.0006) s^{-1} for the 44 kDa fragment. To estimate the amount of variation that would be consistent with the experimental errors in the values of k_2, the same fitting procedure was also carried out using $k_2 + \sigma(k_2)$ and $k_2 - \sigma(k_2)$ in place of k_2; this yielded ranges of values for k_3 of 0.0031−0.0045 and 0.0047−0.0061 s^{-1} for hsc70 and the 44 kDa fragment, respectively.

For both hsc70 and the ATPase fragment, the measured off-rate constant for P_i is substantially slower than the off-rate constant for ADP. Also, the P_i inhibition of ADP release has suggested that, to a good approximation, product release is ordered. Consequently, we would expect that, under identical buffer conditions, the observed off-rate for ADP should be slower for a protein that initially has P_i bound than for a protein that does not. We have tested this suggestion by measuring the rate of release of [α-^{32}P]ADP from (1) protein initially incubated in 1.0 mM P_i and then rapidly diluted 20-fold to 50 μM P_i as compared directly to (2) protein both incubated in, and diluted into, 50 μM P_i (Figure 5). We observe that for protein initially incubated in higher $[P_i]$, the apparent ADP release rate is slower than for protein maintained in 50 μM P_i throughout the experiment. The K_d for P_i is not known with precision; however, it can be estimated from the P_i inhibition of ADP release as being on the order of ~1 mM, since the presence of 50 μM P_i shows no inhibition of ADP release, but 1 mM P_i results in substantial inhibition (Figure 1b). Hence, we are diluting from conditions of partial P_i occupancy on the protein at equilibrium to conditions of essentially complete dissociation. The slower apparent release of ADP under these conditions is qualitatively consistent with the ordered release of

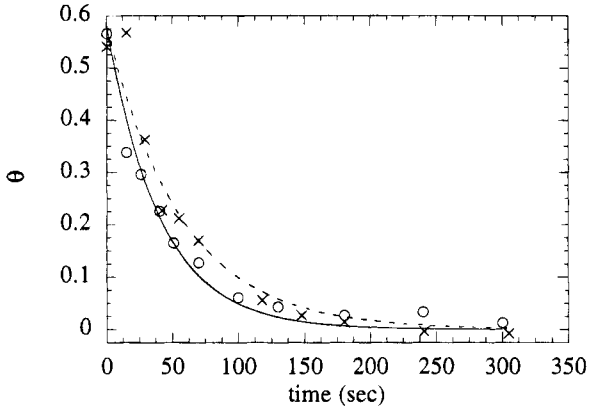

FIGURE 5: Effect of P_i on ADP release from the 44 kDa fragment. θ denotes the fraction of background-corrected radioactive counts from [α-^{32}P]ADP retained on the filter. (×) Protein was initially in 1 mM P_i and was then diluted to give a final concentration of 50 μM P_i. The dashed curve is drawn for clarity and does not represent a fit of the function to the data. (○) protein was initially in 50 μM P_i and was diluted to the same concentration of P_i.

products, where P_i is released first with a slower off-rate, followed by ADP with a faster off-rate.

Steady-State ATPase Parameters. The rate of production of MgADP from MgATP was determined under steady-state conditions. For the 44 kDa ATPase fragment, enzyme velocity was measured over the range 0.2−6.4 μM ATP (Figure 6a); these data give $k_{cat}^{ss} = 0.0023$ (±0.0002) s^{-1} and $K_M^{ss} = 0.37$ (±0.09) μM. For hsc70, enzyme velocity was measured at substrate concentrations greater than K_M^{ss}, in the range 9−96 μM (Figure 6b), giving $k_{cat}^{ss} = 0.0012$ (±0.0002) s^{-1}. Similar measurements were made to determine the steady-state turnover numbers in 25 mM KCl/10 mM $(NH_4)_2SO_4$ buffer, yielding values for k_{cat}^{ss} of 0.000 66 (±0.000 03) s^{-1} for hsc70 and 0.000 91 (±0.000 05) s^{-1} for the ATPase fragment under these conditions. Both of these values are approximately 2-fold lower than the corresponding values determined in the 75 mM KCl buffer.

The steady-state turnover numbers provide a check of the overall consistency of the kinetic constants determined from pre-steady-state experiments. Under steady-state conditions, the initial rate of MgADP formation (for k_{-4}[ADP] $\approx$ 0) can be parametrized:

$$k_{cat} = \frac{k_2k_3k_4}{(k_2 + k_{-2})(k_{-3}[P_i] + k_4) + k_3(k_2 + k_4)} \quad (12)$$

Since the chemical hydrolysis step is essentially irreversible, $k_{-2} \ll k_2$. Under our conditions, where measurement of the initial rate of MgADP formation is restricted further to where $k_{-3}[P_i] \ll k_4$, then this expression reduces to

$$k_{cat}^{ss} = \frac{k_2k_3k_4}{k_2k_3 + k_2k_4 + k_3k_4} \quad (13)$$

The values of k_{cat}^{ss} computed from the measured values of k_2, k_3, and k_4 are 0.0016 (±0.0002) s^{-1} for hsc70 and 0.0034 (±0.0003) s^{-1} for the 44 kDa fragment. These numbers are approximately 30% and 40% larger than the measured values of k_{cat}^{ss} for hsc70 and the 44 kDa fragment, respectively, and hence the differences between measured and calculated steady-state turnover rates are approximately twice as large as the sum of their standard deviations. There are two

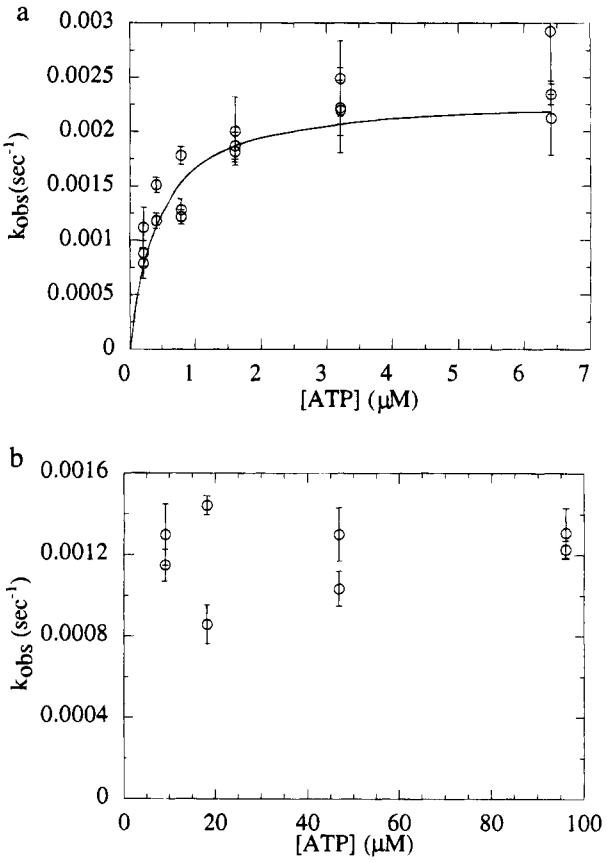

FIGURE 6: Steady-state ATPase kinetics. Dependence of k_{obs} of MgATP hydrolysis determined from steady-state experiments on the concentration of ATP for (a) 0.02 μM 44 kDa fragment and (b) 0.42 μM hsc70. k_{obs} is obtained by dividing initial velocity by an enzyme concentration. The uncertainty associated with k_{obs} is the standard error of the linear least-squares fit as a function of time. Curves represent weighted nonlinear least-squares fits of a hyperbolic function (eq 2) to k_{obs}.

plausible contributions to this discrepancy. The first is that the statistical errors underestimate the cumulative systematic errors of the measurements, in which case a discrepancy of ~30−40% would not be unexpected for numbers whose relative standard deviations are ~10%. The second is that the value of the steady-state turnover, which is computed as an enzyme velocity divided by the total enzyme concentration, is susceptible to being underestimated if the enzyme is less than 100% active in MgATP hydrolysis, while the individual rate constants that are determined under pre-steady-state conditions with enzyme in large excess over substrate are less susceptible to systematic underestimation due to low activity.

DISCUSSION

We have carried out a series of kinetic and equilibrium binding experiments to determine the rate constants of the individual steps of the ATPase cycle for both recombinant bovine hsc70 and its 44 kDa ATPase fragment. We have interpreted our data using an enzymatic cycle with ordered product release (Scheme 1), in which the release of P_i precedes that of ADP; the P_i-dependent inhibition of ADP release supports this as a reasonable approximation. Inhibition of ADP release by P_i has previously been reported for bovine hsc70 (Gao et al., 1993). We also set $k_{-2} \approx 0$ in Scheme 1 and approximate the hydrolysis step as essentially irreversible, since we have been unable to observe the

synthesis of MgATP from MgADP and P_i under any experimental conditions we have tried. This is not unexpected in light of the structural work on the 44 kDa ATPase fragment, which has revealed both the conformation in which MgATP or nonhydrolyzable ATP analogs bind prior to hydrolysis and the conformation of MgADP + P_i after hydrolysis (Flaherty et al., 1994). A major difference between the two states is that the P_i in the posthydrolysis state is ~3.4 Å away from the position of the γ-phosphate of ATP before hydrolysis. Therefore, the leaving phosphate must move substantially during the course of hydrolysis, and it is not surprising that the reverse reaction, which might be favorable if the final product state were sterically close to the transition state, is strongly disfavored in this case. Finally, although hsc70 is known to undergo conformational changes during the course of its ATPase cycle (Liberek et al., 1991b; Palleros et al., 1992), which might enter in as additional intermediates in the cycle, we have not attempted to describe multiple conformations or correlate transition rates between different conformations with steps in the enzymatic cycle at this time.

hsc70 and the 44 kDa ATPase fragment are quantitatively similar in their interactions with MgADP; their measured equilibrium binding constants for MgADP are equal within experimental error, as are their measured ADP release rates. For hsc70, the MgATP on- and off-rates were also measured. The on-rates for MgATP and MgADP are essentially equal, while the off-rate is approximately 2.5 times faster for ADP than for ATP, resulting in a ~2.5-fold weaker binding affinity of MgADP for hsc70. The ADP release rate was also measured in 25 mM KCl/10 mM $(NH_4)_2SO_4$ for hsc70 and found to be unchanged from the value measured in 75 mM KCl.

Previous values reported for equilibrium dissociation constants for ADP or ATP from hsc70 range from $\sim 10^{-5}$ to $\sim 10^{-8}$ M. Using bovine hsc70 at a concentration of ~1 μM, early measurements by Schmid et al. (1985) reported K_d(MgADP) = 1.35 μM with binding stoichiometry not determined and K_d(MgATP) = 0.7 μM with 0.4 nucleotide per protein, measured in 75 mM KCl and 4.5 mM Mg^{2+}. However, no steps were taken to remove bound nucleotide from the protein prior to the addition of labeled nucleotide; the reported values may be distorted by residual bound nucleotide. Palleros and Fink (1991) reported K_d(ATP) = 9.5 μM and K_d(ADP) = 1.6 μM for bovine hsc70 in 200 mM KCl and 20 mM sodium phosphate buffer. The apparently weaker binding, as compared to other reported values, may be due to the absence of Mg^{2+} in the experiment, which specifically coordinates nucleotides in their complexes with hsc70. The higher apparent affinity for ADP, relative to ATP, may be due to P_i inhibition of ADP release. Wang and Lee (1993) report K_d(MgATP) ~ 0.2−0.3 μM for recombinant bovine hsc70 in 120 mM NaCl and 5 mM Mg^{2+}, with a measured stoichiometry of 0.4 MgATP/hsc70; efforts were not taken to discriminate between MgATP and MgADP in the experiments. These values differ slightly from those reported here; this may be due to differences in the methods employed to remove nucleotide prior to binding experiments or to the weaker binding of nucleotides to hsc70 in the presence of Na^+ as opposed to K^+ (M. C. O'Brien and D. B. McKay, personal communication). Gao et al. (1994) report values of K_d(MgATP) = 0.012 μM and K_d(MgADP) = 0.018 μM for bovine hsc70, measured by competition with MgAMPPNP in 25 mM KCl/10 mM $(NH_4)_2SO_4$ buffer. Although the values are somewhat lower than those reported here for recombinant hsc70, K_d^{calcd}(MgATP) = 0.042 ± 0.007 μM and K_d(MgADP) = 0.11 ± 0.02 μM, the discrepancy may result either from differences in the experimental methods used to determine the values or from in an intrinsic difference between natural bovine and recombinant protein such as might arise from posttranslational modification, which has been observed *in vivo* in other 70 kDa heat shock proteins (Loomis et al., 1982; Carlsson & Lazarides, 1983; Rieul et al., 1987; Hendershot et al., 1988).

The P_i release rates for hsc70 and the 44 kDa fragment were determined and found to be almost equal. From the P_i inhibition of ADP release for the 44 kDa fragment, we have estimated $K_d(P_i) \sim 1$ mM; this gives $k_{-3} = k_3/K_d(P_i) \sim 1-10$ M^{-1} s^{-1} as an order-of-magnitude estimate of the P_i on-rate. [We have not determined k_{-3} directly, since attempting to do so by filter binding would require inordinately high ($\sim 10^{-4}$ M) protein concentrations and inordinately long ($> 10^4$ s) measurement times or low protein concentrations and labeled P_i in large molar excess over protein, making the results dubious]. The slow off-rate and slow estimated on-rate for P_i require a high free energy barrier between the protein-bound and solution states of P_i. This is consistent with the fact that, in the three-dimensional structure of the wild-type ATPase fragment, bound P_i is completely inaccessible to solvent; to bind, a negatively charged P_i ion must bury itself within the protein.

The rate of chemical hydrolysis, k_2, was measured under single-turnover conditions and found to be severalfold slower for hsc70 than for the ATPase fragment. In hsc70, the rate of hydrolysis, 0.0030 s^{-1}, is similar in magnitude to the computed rate of P_i release, 0.0038 s^{-1}. In contrast, the rate of ADP release, 0.029 s^{-1}, is an order of magnitude more rapid than either of these steps. Under conditions where MgATP binding is relatively rapid, therefore, ATP hydrolysis and P_i release will contribute equally to the steady-state turnover time of the ATPase cycle, while ADP release will make only a minor contribution.

We have also measured the hydrolysis rate constant, k_2, in 25 mM KCl/10 mM $(NH_4)_2SO_4$ for both hsc70 and the 44 kDa fragment. In both cases, the rates are approximately 4-fold slower than the corresponding rates in 75 mM KCl, and there is a concomitant decrease in the steady-state ATPase rates, as expected. The effect of the lower KCl concentration is exerted primarily on the rate of MgATP hydrolysis rather than on the rate of product release. Our steady-state turnover rate for hsc70 at 25 °C in 25 mM KCl/10 mM $(NH_4)_2SO_4$ buffer, 0.000 66 s^{-1}, agrees reasonably well with the rate reported in an abstract by Gao et al. (1992) of 0.0008 s^{-1}. Under the 25 mM KCl buffer conditions, the MgATP hydrolysis step is likely to be the slowest step in the ATPase cycle for hsc70, as Gao et al. (1993) observed.

In the 75 mM KCl buffer, the ATP hydrolysis step is substantially more rapid for the 44 kDa ATPase fragment than for hsc70; consequently, P_i release is the rate-limiting step in the ATPase cycle for the 44 kDa fragment. In this context, it is interesting to note the schematic similarity between the hsc70 ATPase fragment and actin, whose three-dimensional structure is similar (Flaherty et al., 1991). Once MgATP−actin condenses into filaments (F-actin), MgATP hydrolysis is irreversible and has a minimum average rate

on the order of ~0.02−0.05 s^{-1} (Carlier et al., 1984; Pollard & Weeds, 1984) [we note parenthetically that a model in which MgATP hydrolysis by F-actin is highly localized in the filament and much more rapid has also been presented (Pantaloni et al., 1985)]. Subsequent P_i release is significantly slower, with a rate of ~0.005 s^{-1} (Carlier & Pantaloni, 1986). Filaments of MgADP−actin are relatively unstable, allowing the dissociation of actin; thus, MgATP binding switches actin into a state that favors filament formation, while P_i release induces an actin state that favors filament disassembly (Carlier, 1992).

hsc70 and its *E. coli* counterpart, dnaK, are known to cycle between at least two distinct conformations, one of which has a high affinity for peptides and denatured proteins and the other of which has a much weaker affinity. It has been demonstrated that complexes of denatured proteins with hsc70 or dnaK dissociate rapidly upon the addition of MgATP, suggesting that MgATP binding induces peptide release (Palleros et al., 1993; Prasad et al., 1994), to wit the transition from the high peptide affinity state to the low peptide affinity state. In view of the striking similarities in both structure and ATPase kinetics between actin and the 44 kDa ATPase fragment of hsc70, it will be interesting to determine whether the converse transition from the low peptide affinity state to the high peptide affinity state in hsc70 is induced by P_i release, in analogy to the transition from the filament-stable state to the filament-unstable state that is induced by P_i release in actin.

The kinetic difference between recombinant full-length hsc70 and the 44 kDa ATPase fragment under our experimental conditions is primarily due to the substantial difference in the rate of hydrolysis of MgATP. It is noteworthy in this context that the steady-state ATPase rate of recombinant hsc70 can be stimulated at least 2-fold by specific peptides to a level approximately equal to the peptide-independent turnover rate of the 44 kDa fragment; it will be of interest to determine whether the effect of peptide stimulation is primarily on the MgATP hydrolysis step. Characterization of the kinetics of the ATPase cycle for hsc70 protein provides a foundation for future work on correlating the kinetics of peptide binding/release and conformational change with individual steps of the ATPase reaction.

ACKNOWLEDGMENT

We thank Drs. Dan Herschlag, Sigurd Wilbanks, Melanie O'Brien, and Heinz Pley for constructive discussions of this work. We thank Deborah Lindes and Sigurd Wilbanks for assistance in purifying proteins. We thank Drs. Matthew Todd and George Lorimer for their advice on the preparation of [α-^{32}P]ADP.

REFERENCES

Becker, J., & Craig, E. A. (1994) *Eur. J. Biochem. 219*, 11−23.

Beckmann, R. P., Mizzen, L. A., & Welch, W. J. (1990) *Science 248*, 850−854.

Beckmann, R. P., Lovett, M., & Welch, W. J. (1992) *J. Cell Biol. 117*, 1137−1150.

Blond-Elguindi, S., Cwirla, S. E., Dower, W. J., Lipshutz, R. J., Sprang, S. R., Sambrook, J. F., & Gething, M. J. (1993) *Cell 75*, 717−728.

Bork, P., Sander, C., & Valencia, A. (1992) *Proc. Natl. Acad. Sci. U.S.A. 89*, 7290−7294.

Carlier, M.-F. (1992) *Philos. Trans. R. Soc. London B 336*, 93−97.

Carlier, M.-F., & Pantaloni, D. (1986) *Biochemistry 25*, 7789−7792.

Carlier, M.-F., Pantaloni, D., & Korn, E. D. (1984) *J. Biol. Chem. 259*, 9983−9986.

Carlsson, L., & Lazarides, E. (1983) *Proc. Natl. Acad. Sci. U.S.A. 80*, 4664−4668.

Chappell, T. G., Welch, W. J., Schlossman, D. M., Palter, K. B., Schlesinger, M. J., & Rothman, J. E. (1986) *Cell 45*, 3−13.

Chappell, T. G., Konforti, B. B., Schmid, S. L., & Rothman, J. E. (1987) *J. Biol. Chem. 262*, 746−751.

Chirico, W. J., Waters, M. G., & Blobel, G. (1988) *Nature 332*, 805−810.

Deshaies, T. J., Koch, B. D., Werner-Washburne, M., Craig, E. A., & Schekman, R. (1988) *Nature 332*, 800−805.

Flaherty, K. M., DeLuca-Flaherty, C., & McKay, D. B. (1990) *Nature 346*, 623−628.

Flaherty, K. M., McKay, D. B., Kabsch, W., & Holmes, K. C. (1991) *Proc. Natl. Acad. Sci. U.S.A. 88*, 5041−5045.

Flaherty, K. M., Wilbanks, S. M., DeLuca-Flaherty, C., & McKay, D. B. (1994) *J. Biol. Chem. 269*, 12899−12907.

Flynn, G. C., Pohl, J., Flocco, M. T., & Rothman, J. E. (1991) *Nature 353*, 726−730.

Gao, B., Eisenberg, E., & Greene, L. E. (1992) *Mol. Biol. Cell 3S*, 58a.

Gao, B., Emoto, Y., Greene, L., & Eisenberg, E. (1993) *J. Biol. Chem. 268*, 8507−8513.

Gao, B., Greene, L., & Eisenberg, E. (1994) *Biochemistry 33*, 2048−2054.

Gaut, J. R., & Hendershot, L. M. (1993) *J. Biol. Chem. 268*, 7248−7255.

Gething, M. J., & Sambrook, J. (1992) *Nature 355*, 33−45.

Hendershot, L. M., Ting, J., & Lee, A. S. (1988) *Mol. Cell. Biol. 8*, 4250−4256.

Hendrick, J. P., & Hartl, F.-U. (1993) *Annu. Rev. Biochem. 62*, 349−384.

Huang, S., Tsai, M.-Y., Tzou, Y.-M., Wu, W., & Wang, C. (1993) *J. Biol. Chem. 268*, 2063−2068.

Johnson, K. A. (1986) in *Methods in Enzymology* (Vallee, R. B., Ed.) Vol. 134, pp 677−705, Academic Press, Orlando, FL.

Landry, S. J., Jordan, R., McMacken, R., & Gierasch, L. M. (1992) *Nature 355*, 455−457.

Liberek, K., Marszalek, J., Ang, D., Georgopoulos, C., & Zylicz, M. (1991a) *Proc. Natl. Acad. Sci. U.S.A. 88*, 2874−2878.

Liberek, K., Skowyra, D., Zylicz, M., Johnson, C., & Georgopoulos, C. (1991b) *J. Biol. Chem. 266*, 14491−14496.

Loomis, W., Wheeler, S., & Schmidt, J. (1982) *Mol. Cell. Biol. 2*, 484−489.

McKay, D. B. (1993) *Adv. Protein Chem. 44*, 67−98.

McKay, D. B., Wilbanks, S. M., Flaherty, K. M., Ha, J.-H., O'Brien, M. C., & Shirvanee, L. L. (1994) in *The Biology of Heat Shock Proteins and Molecular Chaperones*, pp 153−177, Cold Spring Harbor Laboratory Press, Cold Spring Harbor, NY.

Milarski, K. L., & Morimoto, R. I. (1989) *J. Cell Biol. 109*, 1947−1962.

Murakami, H., Pain, D., & Blobel, G. (1988) *J. Cell Biol. 107*, 2051−2057.

O'Brien, M. C., & McKay, D. B. (1993) *J. Biol. Chem. 268*, 24323−24329.

O'Sullivan, W. J. (1969) in *Data for Biochemical Research*, 2nd ed., pp 423−434, Oxford University Press, New York.

Palleros, D. R., Welch, W. J., & Fink, A. L. (1991) *Proc. Natl. Acad. Sci. U.S.A. 88*, 5719−5723.
Palleros, D. R., Reid, K. L., McCarty, J. S., Walker, G. C., & Fink, A. L. (1992) *J. Biol. Chem. 267*, 5279−5285.
Palleros, D. R., Reid, K. L., Shi, L., Welch, W. J., & Fink, A. L. (1993) *Nature 365*, 664−666.
Pantaloni, D., Hill, T. L., Carlier, M.-F., & Korn, E. (1985) *Proc. Natl. Acad. Sci. U.S.A. 82*, 7207−7211.
Pollard, T. D., & Weeds, A. G. (1984) *FEBS Lett. 170*, 94−98.
Prasad, K., Heuser, J., Eisenberg, E., & Greene, L. (1994) *J. Biol. Chem. 269*, 6931−6939.
Rieul, C., Cortay, J. C., Bleicher, F., & Cozzone, A. J. (1987) *Eur. J. Biochem. 168*, 621−627.
Sadis, S., & Hightower, L. E. (1992) *Biochem*istry *31*, 9406−9412.
Schlossman, D. M., Schmid, S. L., Braell, W. A., & Rothman, J. E. (1984) *J. Cell Biol. 99*, 723−733.
Schmid, S. L., & Rothman, J. E. (1985) *J. Biol. Chem. 260*, 10044−10049.
Schmid, D., Baici, A., Gehring, H., & Christen, P. (1994) *Science 263*, 971−973.
Schmid, S. L., Braell, W. A., & Rothman, J. E. (1985) *J. Biol. Chem. 260*, 10057−10062.
Sheffield, W. P., Shore, G. C., & Randall, S. K. (1990) *J. Biol. Chem. 265*, 11069−11076.
Wang, C., & Lee, M. R. (1993) *Biochem. J.* 69−77.
Wilbanks, S. M., DeLuca-Flaherty, C., & McKay, D. B. (1994) *J. Biol. Chem. 269*, 12893−12898.